

# Analysis of Energy Detection with Noise Uncertainty over $\alpha$ - $\eta$ - $\kappa$ - $\mu$ Fading Channel

Vanessa Mendes Rennó, Rausley A. A. de Souza, *Member, IEEE*, and Michel Daoud Yacoub, *Member, IEEE*,

**Abstract**—One of the main challenges in implementing spectrum sensing techniques concerns the system robustness against noise power uncertainties. In this paper, a performance analysis of energy detection-based cognitive radio system is carried out assuming absence/presence of noise uncertainty for the sensing channel modeled by the  $\alpha$ - $\eta$ - $\kappa$ - $\mu$  fading channel. The detection capacity of spectral sensing over several representative scenarios is analyzed with the theoretical results validated through Monte Carlo simulations. The results show that the performance of the spectral sensing technique is drastically affected by the noise uncertainty as well as by the channel conditions described the fading parameters  $\alpha$ ,  $\eta$ ,  $\kappa$ , and  $\mu$ . Both the ratio of the power of the dominant component to the power of the scattered and quadrature scattering signal and the clustering imbalance have a smaller impact on the overall performance. The offered results are especially useful in assessing the effect of fading in energy detector-based cognitive radio communication systems.

**Index Terms**—Spectrum sensing, energy detector,  $\alpha$ - $\eta$ - $\kappa$ - $\mu$  fading model, noise uncertainty.

## I. INTRODUCTION

WITH the exponential increase in demand for mobile communications services, the electromagnetic spectrum of radio frequencies tends to become increasingly congested. Regulatory agencies have used fixed band allocation policy, where the resource is allocated by type of service and users acquire the right to exploit certain bandwidth. This management policy results in underutilization of the resource, since the holder of the right to use a particular band may not do it all time and in all area where the service is offered. Consequently, there is a contradictory scenario in which the resource is at the same time scarce and underutilized, generating a great challenge for future mobile technologies, for example 5G and beyond. In this context, the concept of cognitive radio (CR) [2] arises, which proposes, among other functionalities, the opportunistic use of the spectrum. To perform this task, CR carries out the spectral sensing [2], which consists of

collecting samples of a signal in a given bandwidth to infer about its availability. If the sensing band is being occupied by the holder of the right to use it, called primary user (PU), the CR should search for another available band or limit its transmission power to a level of interference acceptable to PU. If the targeted band is idle, CR can use it opportunistically.

There is a great number of spectral sensing techniques proposed in the literature to detect the presence of the signal in a given band. This includes the classic likelihood ratio test (LRT) [3], the energy detector (ED) [3], [4], matched filtering (MF)-based methods [3], cyclostationary detection (CSD) method [5], eigenvalue-based sensing [6] and covariance based sensing [7]. These methods have different requirements and advantages/disadvantages. However, for many detection methods, the noise power is assumed to be known *a priori*. Nevertheless, the change of noise power affects their performance. In practice, noise power does change with time and location, a phenomenon known as noise uncertainty. Because of this, the accurate noise power waveform/distribution is unknown, which affects the performance of detection methods in spectral sensing [8]–[14].

One of the elements in a wireless transmission system that affects the performance of spectral sensing is the communication channel. Concerning the short-term fading, the complex model  $\alpha$ - $\eta$ - $\kappa$ - $\mu$  [15] is of particular interest, for it takes into account all the important small-scale phenomena known to date. Specifically, the model considers the nonlinearity phenomenon of the transmission medium, the power of the scattered waves, the power of the dominant components, and the multipath clustering. In order to impinge some degree of correlation between in-phase and quadrature, imbalances between these two components are inserted [15]. The model has been described by means of its envelope and phase probability density functions (PDFs), which are written in terms of physically-based parameters. It is noteworthy that the said model comprises all of the most relevant fading scenarios found in the literature. Because of its newness as well as comprehensiveness, several issues remain to be explored and investigated, thus creating an enormous opportunity for future researches. Some theoretical or practical studies have already been published in the literature focusing on the  $\alpha$ - $\eta$ - $\kappa$ - $\mu$  model [16]–[19]. Also, algorithms have already been proposed for the generation of uncorrelated  $\alpha$ - $\eta$ - $\kappa$ - $\mu$  samples [20], [21].

The spectrum sensing in fading channels has been studied, for instance, in [2], [22]–[29] and some analyzes were performed in the presence of noise uncertainty [30]–[32], using an energy detection scheme. However, studies regarding generalized fading channels which describe scenarios not covered

Vanessa Mendes Rennó and Rausley A. A. de Souza, National Institute of Telecommunications (Inatel), Santa Rita do Sapucaí - MG - Brazil (Tel:+55 (35) 3471 9227, e-mail: vanessamendes@get.inatel.br, rausley@inatel.br).

Michel Daoud Yacoub, School of Electrical and Computation Engineering, State University of Campinas (Unicamp), Campinas - SP - Brazil, e-mail: michel@decom.fee.unicamp.br.

This work was supported in part by CNPq under Grant 308365/2017-8 and 304248/2014-2, and by RNP, with resources from MCTIC, Grant No. 01250.075413/2018-04, under the Radiocommunication Reference Center (Centro de Referência em Radiocomunicações - CRR) project of the National Institute of Telecommunications (Instituto Nacional de Telecomunicações - Inatel), Brazil.

A shorter conference-type version of this paper was presented in the XXXVI Simpósio Brasileiro de Telecomunicações e Processamento de Sinais (SBtT 2018), Campina Grande, PB, Brazil, September 16-19, 2018 [1].

Digital Object Identifier: 10.14209/jcis.2019.18

by most common fading distributions are still scarce, if not absent, in the literature.

This paper investigates the spectral sensing performance by means of the energy detection technique for the sensing channel described by the envelope of the  $\alpha$ - $\eta$ - $\kappa$ - $\mu$  model, in the absence and presence of noise uncertainty.

This article is organized as follows: in Section II a brief review of the  $\alpha$ - $\eta$ - $\kappa$ - $\mu$  fading model is made. The Section III describes the system model adopted for spectral sensing and the Section IV describes the statistics adopted in the presence of noise uncertainty. In the Section V a study is made on the performance metrics adopted. The numerical results and their interpretations are detailed in Section VI. Finally, Section VII presents the conclusions of this work.

## II. THE $\alpha$ - $\eta$ - $\kappa$ - $\mu$ FADING MODEL

The  $\alpha$ - $\eta$ - $\kappa$ - $\mu$  fading model proposed in [15] accounts for virtually all relevant small-scale propagation phenomena described in the literature, namely, nonlinearity of the medium, power of the scattered waves, power of the dominant components, and multipath clustering.

The resulting phase-envelope joint PDF is presented in three different parametrizations, namely Raw, Local, and Global. In the Global Parametrization [15, Eq. (14)], which is the one applied here, the following are the corresponding physical parameters: (i)  $\alpha > 0$  - the non-linearity of the transmission medium; (ii)  $\eta > 0$  - the ratio of the total power of the in-phase and quadrature scattered waves of the multipath clusters; (iii)  $\kappa > 0$  - the ratio of the total power of the dominant components and the total power of scattered waves; (iv)  $\mu > 0$  - the total number of multipath clusters; (v)  $q > 0$  - the ratio of two ratios: the ratio of the power of the dominant components to the ratio of the power of the scattered waves of the in-phase signal and its counterpart for the quadrature signal; (vi)  $p > 0$  - the ratio of the number of multipath clusters of in-phase and quadrature signals; (vii)  $\hat{r}^\alpha > 0$ , - the mean value  $\mathbb{E}(R^\alpha)$ , for a fading signal with envelope  $R$ .

It is noteworthy that, in [15], and for the envelope, an exact, fast-convergent series expansion for its PDF and also for its cumulative distribution function (CDF) are found. Additionally, in [15] the reader can find some important joint PDFs for the envelope-based and for the complex fading model.

A great number of well-known distributions, and others not yet available in the literature, can be obtained as particular cases of the  $\alpha$ - $\eta$ - $\kappa$ - $\mu$  fading model [15, Section VI]. Fig. 1 shows a detailed relationship between the parameters of the  $\alpha$ - $\eta$ - $\kappa$ - $\mu$  distribution and known distributions as its special cases. Specifically, the three-fading-parameter distributions ( $\eta$ - $\kappa$ - $\mu$ ,  $\alpha$ - $\kappa$ - $\mu$ ,  $\alpha$ - $\eta$ - $\mu$ , and  $\alpha$ - $\eta$ - $\kappa$ ), the two-fading-parameter distributions ( $\kappa$ - $\mu$ ,  $\eta$ - $\mu$ , Beckmann ( $\eta$ - $\kappa$ ),  $\alpha$ - $\mu$ ,  $\alpha$ - $\kappa$  and  $\alpha$ - $\eta$ ), the one-fading-parameter ones, namely, Nakagami- $m$ , Rice, Hoyt, and Weibull, and no-fading-parameter ones, namely, semi-Gaussian, Rayleigh, and negative exponential. A diagram illustrating the migration of the general envelope-based  $\alpha$ - $\eta$ - $\kappa$ - $\mu$  fading model to its main special cases is shown in Fig. 1. (These are the main transitions. Others involving the parameters  $p$  and  $q$  and specific values of other parameters

not appearing in the diagram were left aside not to pollute the diagram.)

The reader is invited to refer to the seminal paper [15] in order to obtain a detailed description of the  $\alpha$ - $\eta$ - $\kappa$ - $\mu$  fading model, its statistics and the mapping between different parametrization formats.

## III. ENERGY DETECTOR

As far as spectral sensing is concerned, the CR does not have a priori information about the characteristics of the signals to be detected. For these cases, the receiver can be implemented by the ED. The detector will estimate the energy present within the operation frequency range during an observation interval and will compare the result with a threshold  $\lambda$ , that depends on the noise power at the receiver input. If the estimated value is below the threshold, the channel is considered idle, representing a transmission opportunity for the secondary user (SU). Otherwise, the channel is considered busy.

The discrete time model for the hypothesis test associated with spectral sensing can be written as

$$y(\ell) = \begin{cases} n(\ell) & \text{under hypothesis } \mathcal{H}_0 \\ rx(\ell) + n(\ell) & \text{under hypothesis } \mathcal{H}_1. \end{cases} \quad (1)$$

In (1),  $\mathcal{H}_0$  denotes the hypothesis that the channel is idle and  $\mathcal{H}_1$  denotes the busy channel condition,  $y(\ell)$  is the  $\ell$ -th sample,  $\ell = 1, \dots, L$ , of the received signal collected by the CR during the sensing interval,  $x(\ell)$  is a sample of the signal transmitted by the PU and  $r$  represents the envelope of the fading channel, assumed to be flat and static during the sensing interval. The variable  $n(\ell)$  indicates a sample of additive white Gaussian noise (AWGN) with zero mean and variance  $\sigma_{\text{AWGN}}^2 = N_0\mathcal{B}$ , measured in a band  $\mathcal{B}$  with unilateral power spectral density  $N_0$ , generated at the receiver input of CR.

The PU signal to be detected,  $x(\ell)$ , is part of the *unknown deterministic signals* class, initially analyzed in the context of spectral sensing in a non-fading channel in [4] and widely used in later works for performance analysis on fading channels [33], [34]. In this model, the PU signal energy to be detected must be deterministic, although unknown. As an example, this class includes the signals in band-pass modulated by phase shift keying (PSK). All the symbols of this constellation have the same energy and there is no information on the amplitude of the signal. Obviously, other types of signals can be exercised. What changes in this case, is the probability of detection since only this metric is influenced by the PU signal.

From the received signal samples, the test statistic for an ED can be calculated by

$$\mathcal{T} = \frac{1}{\sigma_{\text{AWGN}}^2} \sum_{\ell=1}^L y(\ell)^2. \quad (2)$$

The number of samples  $L$  relates to the sensing interval  $t_{\text{sens}}$  and the band  $\mathcal{B}$  by means of the parameter time-band product, i.e.  $u = t_{\text{sens}}\mathcal{B}$ , resulting in  $L = 2t_{\text{sens}}\mathcal{B}$  [33].

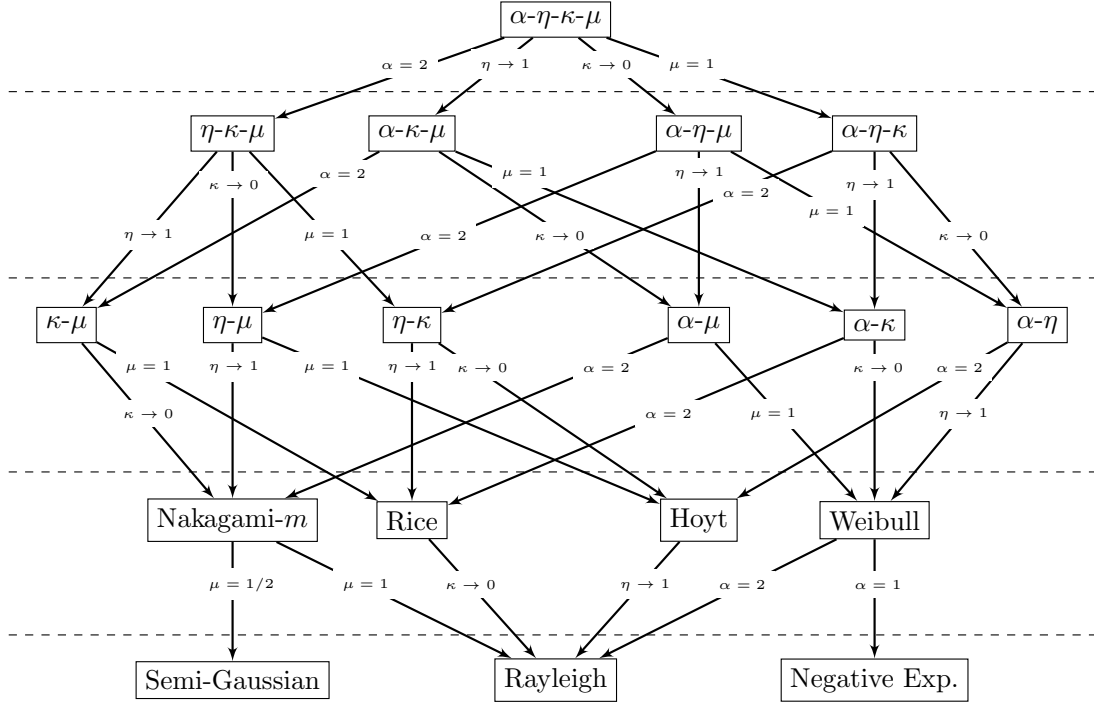


Fig. 1. Relationship between the parameters of the  $\alpha$ - $\eta$ - $\kappa$ - $\mu$  distribution and the distributions with fewer parameters.

The average signal-noise ratio (SNR) follows the definition found in [34], i.e.

$$\bar{\gamma} = \frac{\mathbb{E}[R^2]E_x}{N_0}, \quad (3)$$

where the average energy of the PU signal during the sensing interval is given by  $E_x = \sum_{\ell=1}^L x(\ell)^2 / (2B)$  and  $\mathbb{E}[R^2]$  is the second moment of the  $\alpha$ - $\eta$ - $\kappa$ - $\mu$  fading envelope model. Assuming  $\mathbb{E}[R^2] = 1$  and using  $N_0 = \sigma_{\text{AWGN}}^2 / B$ , the average SNR can be simplified to  $\bar{\gamma} = \sum_{\ell=1}^L x(\ell)^2 / (2\sigma_{\text{AWGN}}^2)$ . If the PU signal has the power  $P_x = E_x / t_{\text{sens}} = \sum_{\ell=1}^L x(\ell)^2 / L$ , the variance (power) of the thermal noise can be determined from the average SNR by applying the ratio

$$\sigma_{\text{AWGN}}^2 = \frac{LP_x}{2\bar{\gamma}}. \quad (4)$$

It is worth mentioning that, in this paper, for convenience, we address the problem for a low-pass process. In the literature [4], [33], it has been extensively verified that both band-pass type and its low-pass equivalent process can be taken interchangeably from the decision statistics perspective. By doing this, systems with different transmission rates, carrier frequencies, and bandwidths can be compared.

#### IV. NOISE POWER UNCERTAINTY

Usually, in detection methods, the thermal noise is assumed to have white Gaussian nature, which is characterized by AWGN. However, in practice, some factors affects the stability of the noise power. On one hand, the variation of temperature at the receiver end leads to the changes of the local thermal

noise power. On the other hand, the environment noise, which is an aggregation of random signals from various sources in the environment, also varies with time. As a result, it is difficult to exactly know the current noise power.

The estimated noise power has a great effect on the performance of some spectrum sensing schemes such as ED [10], [11]. Thus, it is a critical information. In practical scenarios, the noise power is not known in advance and noise uncertainty is always present. Let the estimated noise power be  $\hat{\sigma}_{\text{AWGN}}^2$ . The actual noise power  $\sigma_{\text{AWGN}}^2$  at a given location and time period can be different from the expected one, that is, there is noise power uncertainty. Let  $\hat{\sigma}_{\text{AWGN}}^2 = a\sigma_{\text{AWGN}}^2$ , where  $a$  is the *noise uncertainty factor*. The upper bound of the noise uncertainty factor (in dB) is defined as [12], [13]

$$B = \sup \{10 \log_{10} a\}, \quad (5)$$

where  $B$  is the *noise uncertainty bound*. Let uncertainty bound be described by the uniform distribution, as widely used model in the literature. Then,  $a$  (in dB) is uniformly distributed in the interval  $[-B, B]$  [8], [9]. In practice, the noise uncertainty bound of a receiving device is normally below 2 dB. The noise uncertainty factor  $a$  changes in the interval of  $[10^{-\frac{B}{10}}, 10^{\frac{B}{10}}]$ . The PDF of  $a$  can be found as

$$f_a(a) = \begin{cases} 0 & a < 10^{-\frac{B}{10}} \\ \frac{5}{Ba \log_e(10)} & 10^{-\frac{B}{10}} < a < 10^{\frac{B}{10}} \\ 0 & a > 10^{\frac{B}{10}}. \end{cases} \quad (6)$$

## V. PERFORMANCE METRICS

Sensing performance is commonly measured by the probability of false alarm and by the probability of detection, the former corresponding to the probability that the detector decides in favor of the presence of PU, even though it is not in the sensed band, and the latter corresponding to the probability of the correct detection of an unknown signal, which is actually present in the sensed band.

Based on the test statistic  $\mathcal{T}$  of ED defined in (2) and considering the  $\alpha$ - $\eta$ - $\kappa$ - $\mu$  fading channel, the theoretical probability of false alarm and the probability of detection are calculated for ED as [33]

$$P_{fa} = \Pr\{\mathcal{T} > \lambda \mid \mathcal{H}_0\} = \frac{\Gamma(u, \frac{\lambda}{2})}{\Gamma(u)} \quad (7)$$

and

$$P_d = \Pr\{\mathcal{T} > \lambda \mid \mathcal{H}_1\} = \int_0^\infty Q_u(\sqrt{2\gamma}, \sqrt{\lambda}) f_\Gamma(\gamma) d\gamma, \quad (8)$$

where  $\Pr\{\cdot\}$  is the probability of occurrence of any event,  $\lambda$  is the decision threshold,  $\Gamma(\cdot, \cdot)$  is the upper incomplete Gamma function [35],  $u$  is the time-band product,  $Q_u(\cdot, \cdot)$  is the generalized Marcum-Q function of  $u$ -th order [36],  $\gamma$  is the instantaneous SNR and  $f_\Gamma(\gamma)$  is the PDF of the  $\alpha$ - $\eta$ - $\kappa$ - $\mu$  distribution as a function of  $\gamma$ . One of the possible manners to obtain  $f_\Gamma(\gamma)$  is by applying the transformation of variables  $\Gamma = \bar{\gamma}R^2$  in [15, Eqn. (10)], which results in

$$f_\Gamma(\gamma) = \frac{\alpha\gamma^{\frac{\alpha-2}{2}}}{2\bar{\gamma}^\alpha} \int_0^{\left(\frac{\gamma}{\bar{\gamma}}\right)^{\frac{\alpha}{2}}} f_X\left(\left(\frac{\gamma}{\bar{\gamma}}\right)^{\frac{\alpha}{2}} - y\right) f_Y(y) dy, \quad (9)$$

where the PDFs  $f_X(x)$  and  $f_Y(y)$  are given by [15, Eqn. (2)].

When noise uncertainty is present in the system, the estimated noise power influences the test statistic defined in (2), resulting in an estimated test statistic being  $\hat{\mathcal{T}} = \mathcal{T}/a$ . At the reception end, the estimated test statistic is compared with the decision threshold, that is  $\hat{\mathcal{T}} > \lambda$ , which in terms of the actual test statistic results in  $\mathcal{T} > a\lambda$  [31]. Furthermore, by the definition given in (4), the estimated average SNR will be  $\hat{\gamma} = \bar{\gamma}/a$ , that is, the actual instantaneous SNR relates to the estimated instantaneous SNR as  $\gamma = a\hat{\gamma}$ . Thus, in the presence of noise uncertainty, the probability of false alarm and the probability of detection, considering the influence of the uncertainty factor on the decision threshold and the instantaneous SNR, are obtained by averaging over the noise uncertainty factor as [12]

$$\begin{aligned} P_{fa} &= \int_a f_a(a) P_{fa} da \\ &= \int_{10^{-\frac{B}{10}}}^{10^{\frac{B}{10}}} \frac{5\Gamma(u, \frac{a\lambda}{2})}{Ba \log_e(10)\Gamma(u)} da \end{aligned} \quad (10)$$

and

$$\begin{aligned} P_d &= \int_a f_a(a) P_d da \\ &= \int_{10^{-\frac{B}{10}}}^{10^{\frac{B}{10}}} \int_0^\infty \frac{5Q_u(\sqrt{2a\hat{\gamma}}, \sqrt{a\lambda}) a f_\Gamma(a\hat{\gamma})}{Ba \log_e(10)} d\hat{\gamma} da. \end{aligned} \quad (11)$$

The probability of false alarm and the probability of detection are used to construct the receiver operating characteristic (ROC) curve. It is a two-dimensional graph given by  $P_{fa}$  versus  $P_d$ , as the threshold  $\lambda$  is varied. The performance of the system, analyzed by ROC, is higher as the curve approaches the point (0, 1). However, in this article, a single figure of merit is also used, calculated from ROC, which can provide a better understanding of the overall detection capacity of spectral sensing. This measure is the area under ROC curve (AUC), an alternative metric that does not account for specific values of  $P_{fa}$  and  $P_d$  but the area below ROC. Then, the average AUC, denoted hereafter as  $\overline{AUC}$ , can be evaluated as [37, Eqn. (4)]

$$\overline{AUC} = \int_0^1 P_d dP_{fa}. \quad (12)$$

Since  $P_{fa}$  and  $P_d$  are both functions of the threshold  $\lambda$ , the threshold averaging method [38] can be used in the evaluation of AUC. Noting that  $P_{fa}$  and  $P_d$  varies from  $0 \rightarrow 1$  as  $\lambda$  varies from  $\infty \rightarrow 0$ , (12) can be rewritten as [37, Eqn. (5)]

$$\overline{AUC} = - \int_0^1 P_d \frac{dP_{fa}}{d\lambda} d\lambda. \quad (13)$$

Note that, in both ROC and AUC, the values of  $P_{fa}$  and  $P_d$  are calculated by (7) and (8), in the absence of noise uncertainty, and by (10) and (11), in the otherwise case, considering the  $\alpha$ - $\eta$ - $\kappa$ - $\mu$  fading channel. Several authors have evaluated the performance, numerically or analytically, of the spectral sensing of the ED technique in terms of the AUC, under several types of fading channels [2], [24], [30], [37], [39].

## VI. NUMERICAL RESULTS

Simulation results of the global spectral sensing performance of several scenarios will be assessed in order to verify the influence of the main parameters that characterize the  $\alpha$ - $\eta$ - $\kappa$ - $\mu$  fading model, also considering the influence of SNR and noise uncertainty. The sensing channel is considered slow and therefore is constant within a given sensing interval, varying only between one period and another. For the estimation of each value of  $P_{fa}$  and  $P_d$  for the construction of the ROCs  $10^5$  realizations of the process by Monte Carlo simulation of the spectral sensing have been performed, and also 100 AUCs for the calculation of  $\overline{AUC}$ . The activity of the PU was simulated as a Bernoulli random variable, with 50% of time active, to account for the detections and 50% of time inactive, for the false alarms. The  $\alpha$ - $\eta$ - $\kappa$ - $\mu$  fading channel samples, and its particular cases, were generated as in [20], [21].

In Fig. 2 and Fig. 3, ROC curves are shown, for fixed parameters of the  $\alpha$ - $\eta$ - $\kappa$ - $\mu$  distribution, with different average SNR values and with the absence and presence of noise uncertainty, for different values of noise uncertainty bound  $B$ . The solid lines represent the theoretical results, calculated and solved numerically by (7) and (8) in the absence of noise uncertainty, and by equations (10) and (11), otherwise, and the marks, the simulated results. In Fig. 2 the number of collected samples at a given sensing interval is  $L = 20$  and in Fig. 3,  $L = 30$ . Comparing the two Figures, it can be noticed that a higher value of collected samples  $L$  results in a drop in

performance. Given the definition of SNR adopted in (3), it is seen that an increase in  $L$  will simply result in a degradation of the global performance in terms of ROC and, consequently, AUC. Because all the transmitted PU symbols have the same energy (power) (refer to Section III), notice from (4) that as  $L$  increases, the noise power also increases. Also, when the number of collected samples increases, the detection and false alarm probabilities both increase. Nonetheless, the probability of false alarm increases faster than the probability of detection, leading to a lower overall detection capability, here measured by AUC. This result was already reported in the literature, for instance [33], [37]. In general, for the Figs. 2 and 3, a higher value of average SNR results in an improvement in the sensing performance. On the other hand, in the presence of noise uncertainty the performance of the sensing is always worse, with increased degradation for higher values of  $B$ .

In Figs. 4, 5 and 6, average curves of AUC are shown, in which the symbols are the simulated points and lines the theoretical curves, calculated from equation (13). The  $P_{fa}$  and  $P_d$  values of this equation are calculated by equations (7) and (8) in the absence of noise uncertainty and by equations (10) and (11) otherwise.

In Fig. 4, average curves of AUC are shown as a function of average SNR values, for fixed parameters of the  $\alpha$ - $\eta$ - $\kappa$ - $\mu$  distribution, with different number of collected samples  $L$  and with the absence and presence of noise uncertainty, for different values of noise uncertainty bound  $B$ . It is noted in all situations that for higher values of average SNR always results in a higher  $\overline{AUC}$  values, that is, an improvement in performance of the spectral sensing. In the absence of noise uncertainty, the  $\overline{AUC}$  value is always higher, for any average SNR value, when compared to the presence of noise uncertainty at detection. In these cases, the  $\overline{AUC}$  value is always lower when noise uncertainty bound  $B$  value is greater. Note that for the same set of parameters, a higher value of collected samples  $L$  results in a lower  $\overline{AUC}$  value, that is, a decrease in the sensing performance.

In Fig. 5, curves for  $\overline{AUC}$  are shown as a function of noise uncertainty bound  $B$ , for fixed parameters of the  $\alpha$ - $\eta$ - $\kappa$ - $\mu$  distribution, with different number of collected samples  $L$  and for different values of average SNR. It is observed that for higher values of the noise uncertainty bound  $B$  the  $\overline{AUC}$  value is always lower, that is, the global sensing performance is worse. When  $B = 0$  dB, meaning absence of noise uncertainty, the highest  $\overline{AUC}$  value occurs. It can be noted that for any value of the noise uncertainty bound  $B$ , a higher average SNR value results in higher  $\overline{AUC}$  values and higher value of collected samples  $L$  results in lower  $\overline{AUC}$  values, which means that in the first case an improvement in the sensing performance occurs and in the second case, the opposite occurs.

In Fig. 6, curves for  $\overline{AUC}$  are shown as a function of the parameters  $\alpha$ ,  $\eta$ ,  $\kappa$ ,  $\mu$ ,  $q$  and  $p$  for different values of SNR, in the absence and presence of noise uncertainty. The number of collected samples at a given sensing interval is  $L = 20$  and, in the presence of noise uncertainty, the noise uncertainty bound used is  $B = 2$  dB. For comparison purposes, theoretical curves of some conventional models are also drawn:  $\alpha$ - $\mu$  [2,

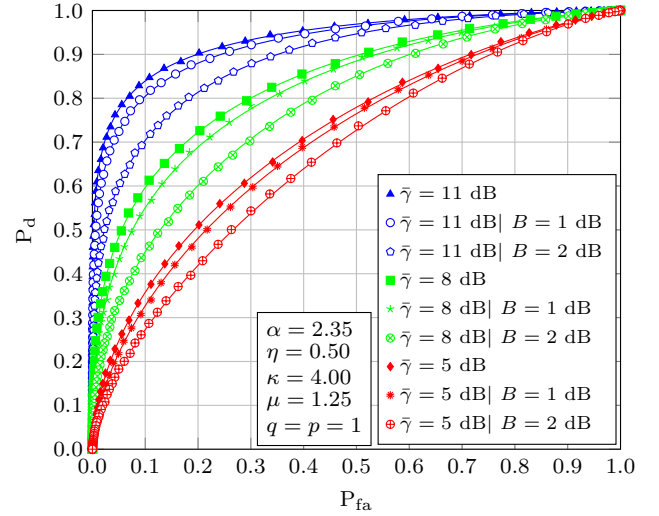


Fig. 2. ROC curves for the  $\alpha$ - $\eta$ - $\kappa$ - $\mu$  fading channel, with different average SNR values, in the absence and presence of noise uncertainty for  $L = 20$ .

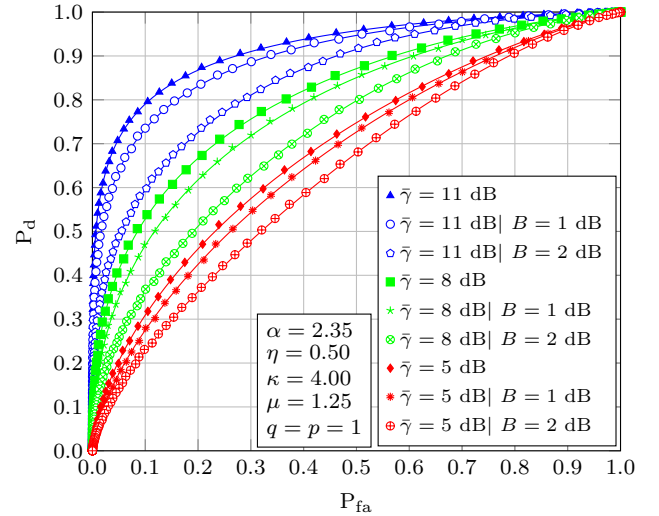


Fig. 3. ROC curves for the  $\alpha$ - $\eta$ - $\kappa$ - $\mu$  fading channel, with different average SNR values, in the absence and presence of noise uncertainty for  $L = 30$ .

Eqn. (48)],  $\eta$ - $\mu$  Format 1 [2, Eqn. (41)],  $\eta$ - $\kappa$  [2, Eqn. (27)] e  $\kappa$ - $\mu$  [2, Eqn. (29)].

For all cases, the sensing performance is worse under the influence of noise uncertainty, that is, lower value of  $\overline{AUC}$ . Regarding the fading parameters, for higher values of  $\alpha$ ,  $\kappa$ , or  $\mu$ , represented respectively in parts (a), (c) and (d) of Fig. 6, more deterministic the channels become, resulting in an improvement in the performance of the sensing, i.e., higher  $\overline{AUC}$  values. This performance improvement will be limited to the case of the evaluation of a system under only the effect of thermal noise. Looking at part (b) of Fig. 6, the optimal performance is reached around  $\eta = 1$ , and minimum values of  $\overline{AUC}$  occur when  $\eta \rightarrow 0$  and  $\eta \rightarrow \infty$ . The overall performance of spectral sensing is more sensitive to variations of the  $\alpha$  parameter, followed by the  $\mu$ ,  $\kappa$ , and  $\eta$  parameters. The unbalance parameters  $q$  and  $p$ , represented in parts (e)

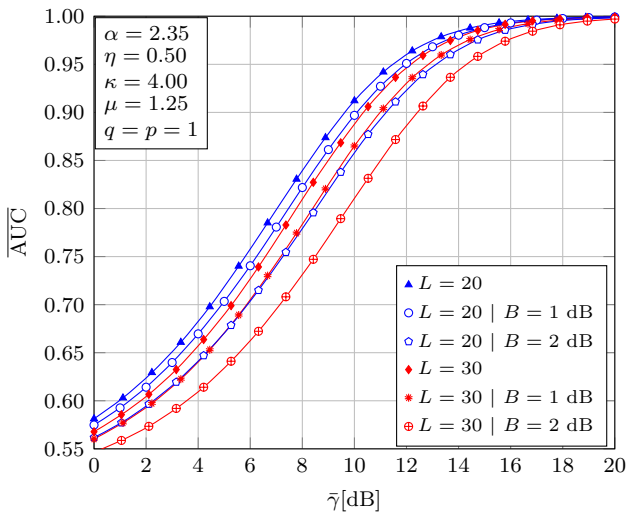


Fig. 4. AUC curves in  $\alpha$ - $\eta$ - $\kappa$ - $\mu$  fading channels as a function of SNR values, in the absence and presence of noise uncertainty, with different values of  $L$ .

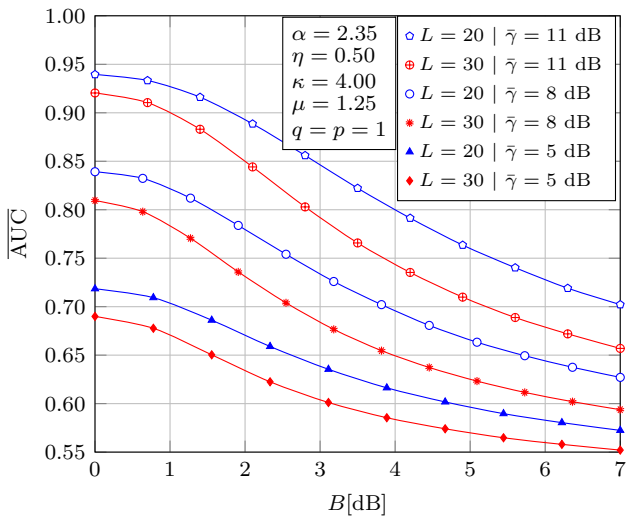


Fig. 5. AUC curves in  $\alpha$ - $\eta$ - $\kappa$ - $\mu$  fading channels as a function of  $B$  values, under different average SNR values and values of  $L$ .

and (f) of Fig. 6, do not significantly affect the  $\overline{\text{AUC}}$ .

It is clear that the inclusion of additional parameters of the  $\alpha$ - $\eta$ - $\kappa$ - $\mu$  model impacts the analysis of system performance decisively. More specifically, the inclusion of the parameters  $\kappa$  and  $\eta$  in the  $\alpha$ - $\mu$  model;  $\alpha$  and  $\kappa$  in  $\eta$ - $\mu$  model;  $\alpha$  and  $\mu$  in  $\eta$ - $\kappa$  model; and  $\alpha$  and  $\eta$  in  $\kappa$ - $\mu$  model. In all of these cases, the difference in performance between the  $\alpha$ - $\eta$ - $\kappa$ - $\mu$  model and the conventional one is greater for higher SNR values. Similarly, this difference in performance is more pronounced for lower values of  $\alpha$ ,  $\kappa$  and  $\mu$ , tending to cancel out to high values of  $\alpha$ ,  $\kappa$  and  $\mu$  since in this scenario the two models tend to become deterministic. In the comparison between the models  $\alpha$ - $\eta$ - $\kappa$ - $\mu$  and  $\eta$ - $\mu$  (Fig. 6(b)), the performances when  $\eta \rightarrow \infty$  are the same when  $\eta \rightarrow 0$ , consequence of the symmetry of the model around  $\eta = 1$  [40].

In parts (e) and (f) of Fig. 6, curves are plotted for  $\eta = 0.5$

and  $\eta = 2$ . Note the symmetry of the performance curves around  $q = 1$  and  $p = 1$ . In general, for a set of parameters  $(\alpha, \eta, \kappa, \mu, p, q)$  has the same performance for  $(\alpha, 1/\eta, \kappa, \mu, p, 1/q)$  or  $(\alpha, 1/\eta, \kappa, \mu, 1/p, q)$ .

## VII. CONCLUSION

This article contributed to the knowledge advancement of the recently proposed  $\alpha$ - $\eta$ - $\kappa$ - $\mu$  distribution. More specifically, the objective was to better understand the influence of the various fading phenomena in the performance of the spectral sensing technique by the ED, in the absence and presence of noise uncertainty. At first, for fixed parameters of the  $\alpha$ - $\eta$ - $\kappa$ - $\mu$  distribution, an analysis of spectral sensing performance was made through ROC and AUC curves for different values of average SNR, with different values of collected samples and in the absence and presence of noise uncertainty, for different values of noise uncertainty bound. For all cases, higher values of average SNR and lower values of collected samples result in an improvement in spectral sensing performance. On the other hand, the presence of noise uncertainty always degrades the performance of the spectral sensing, and more significantly when noise uncertainty bound is higher. In the sequence, the effect of the  $\alpha$ - $\eta$ - $\kappa$ - $\mu$  distribution parameters was analyzed by means of AUC curves. In the several scenarios investigated, the significant impact on the analysis of spectral sensing performance was demonstrated by including the fading parameters  $\alpha$ ,  $\eta$ ,  $\kappa$ , and  $\mu$ . On the other hand, it was observed that both the ratio of the power of the dominant component to the power of the scattered and quadrature scattering signal and the clustering imbalance have a smaller impact on the overall performance. The system model, and consequently the transmitted signal model, adopted was the same one used in [4], [33], [34]. However, based on the information available about the transmitted signal  $x(\ell)$ , the receiver can use other appropriate models that will be useful in analyzing the distribution of the test statistic, as described in (2), under hypothesis  $\mathcal{H}_1$ . Thus, as a possible extension of this work, aiming at a broader approach, and analysis of other models available in the literature can be done, such as those described in [41, Section 2.3.1], to provide more information and complement the conclusions presented here.

## REFERENCES

- [1] V. M. Rennó, R. A. A. de Souza, and M. D. Yacoub, "Original title in portuguese: Análise de desempenho do sensoriamento espectral por detector de energia no canal  $\alpha$ - $\eta$ - $\kappa$ - $\mu$ ," in *XXXVI Brazilian Telecommun. Symp., SBR'T'18*, Sep. 2018.
- [2] P. C. Sofotasios, A. Bagheri, T. A. Tsiftsis, S. Freear, A. Shahzadi, and M. Valkama, "A comprehensive framework for spectrum sensing in non-linear and generalized fading conditions," *IEEE Trans. Veh. Technol.*, vol. 66, no. 10, pp. 8615–8631, Oct. 2017. doi: 10.1109/TVT.2017.2692278
- [3] S. M. Kaye, "Fundamentals of statistical signal processing: Detection theory," 1989.
- [4] H. Urkowitz, "Energy detection of unknown deterministic signals," *Proc. IEEE*, vol. 55, no. 4, pp. 523–531, Apr. 1967. doi: 10.1109/PROC.1967.5573
- [5] W. A. Gardner, "Exploitation of spectral redundancy in cyclostationary signals," *IEEE Signal Process. Mag.*, vol. 8, no. 2, pp. 14–36, Apr. 1991. doi: 10.1109/79.81007

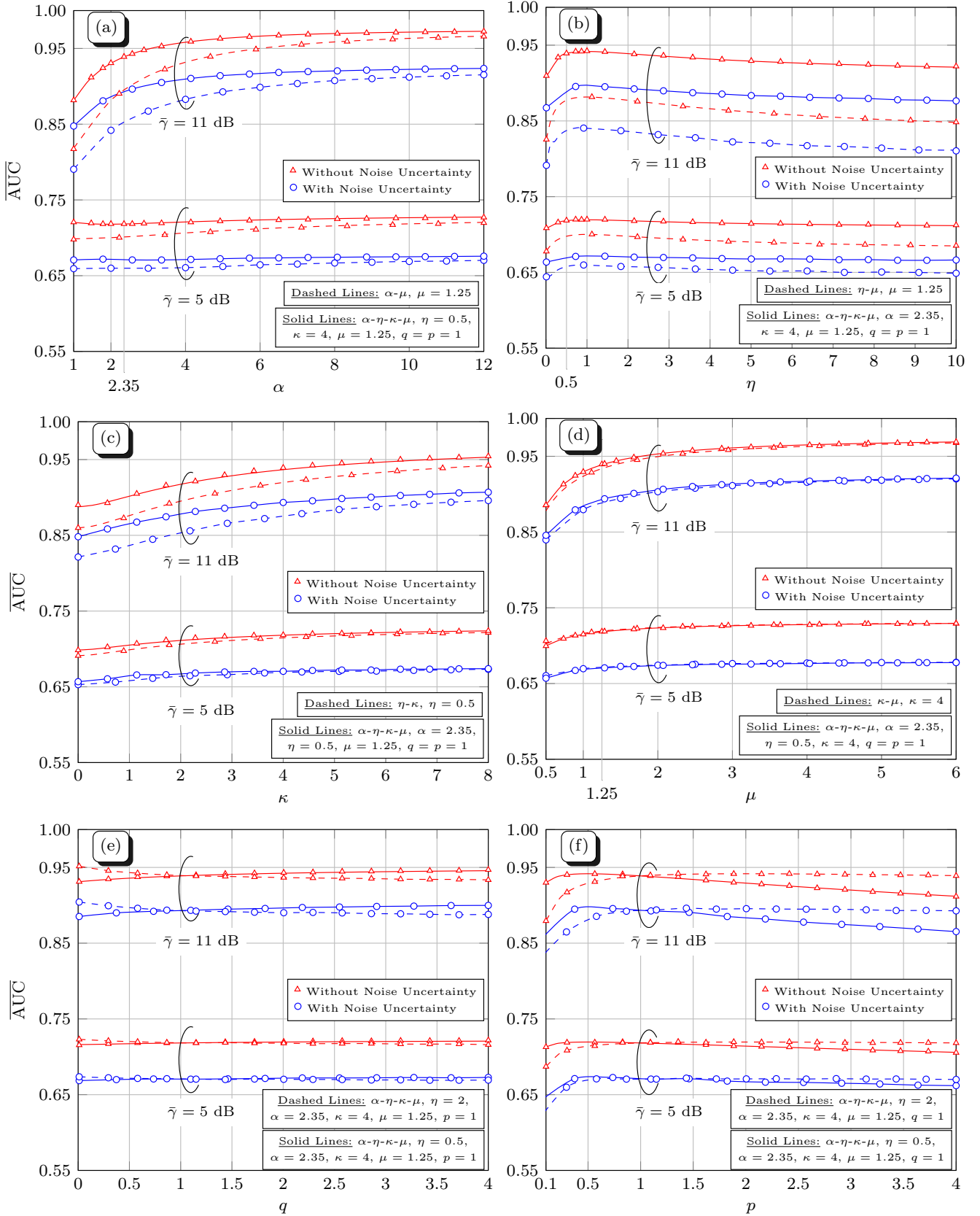


Fig. 6. AUCs of ED in  $\alpha$ - $\eta$ - $\kappa$ - $\mu$  fading channels in the absence and presence of noise uncertainty under different average SNR values as a function of the parameters (a)  $\alpha$ , (b)  $\eta$ , (c)  $\kappa$ , (d)  $\mu$ , (e)  $q$  and (f)  $p$ . For comparison purposes, theoretical curves of some conventional models are also drawn:  $\alpha$ - $\mu$ ,  $\eta$ - $\mu$ ,  $\eta$ - $\kappa$  e  $\kappa$ - $\mu$ .

- [6] Y. Zeng and Y. Liang, "Maximum-minimum eigenvalue detection for cognitive radio," in *IEEE 18th Int. Symp. on Personal, Indoor and Mobile Radio Commun.*, Sep. 2007. doi: 10.1109/PIMRC.2007.4394211. ISSN 2166-9570
- [7] —, "Covariance based signal detections for cognitive radio," in *2nd IEEE Int. Symp. on New Frontiers in Dynamic Spectrum Access Networks*, Apr. 2007. doi: 10.1109/DYSPAN.2007.33
- [8] R. Tandra and A. Sahai, "SNR walls for signal detection," *IEEE J. Sel. Topics Signal Process.*, vol. 2, no. 1, pp. 4–17, Feb. 2008. doi: 10.1109/JSTSP.2007.914879
- [9] Y. Zeng and Y. Liang, "Eigenvalue-based spectrum sensing algorithms for cognitive radio," *IEEE Trans. Commun.*, vol. 57, no. 6, pp. 1784–1793, Jun. 2009. doi: 10.1109/TCOMM.2009.06.070402
- [10] W. Jouini, "Energy detection limits under log-normal approximated noise uncertainty," *IEEE Signal Process. Lett.*, vol. 18, no. 7, pp. 423–426, Jul. 2011. doi: 10.1109/LSP.2011.2155649
- [11] G. Wei, L. Wang, D. Zhang, and S. Zhang, "The effect of noise uncertainty to the performance of energy detection in cooperative detection," in *3rd IEEE Int. Conf. on Broadband Network and Multimedia Tech. (IC-BNMT)*, Oct. 2010. doi: 10.1109/ICBNMT.2010.5705163
- [12] Y. Zeng, Y. Liang, A. T. Hoang, and E. C. Y. Peh, "Reliability of spectrum sensing under noise and interference uncertainty," in *IEEE Int. Conf. on Commun. Workshops*, Jun. 2009. doi: 10.1109/ICCW.2009.5208033. ISSN 2164-7038
- [13] A. Kortun, T. Ratnarajah, M. Sellathurai, Y. Liang, and Y. Zeng, "Throughput analysis using eigenvalue based spectrum sensing under noise uncertainty," in *8th Int. Wireless Commun. and Mobile Computing Conf. (IWCMC)*, Aug. 2012. doi: 10.1109/IWCMC.2012.6314237. ISSN 2376-6492
- [14] J. Tong, M. Jin, Q. Guo, and L. Qu, "Energy detection under interference power uncertainty," *IEEE Commun. Lett.*, vol. 21, no. 8, pp. 1887–1890, Aug. 2017. doi: 10.1109/LCOMM.2017.2705025
- [15] M. D. Yacoub, "The  $\alpha$ - $\eta$ - $\kappa$ - $\mu$  fading model," *IEEE Trans. Antennas Propag.*, vol. 64, no. 8, pp. 3597–3610, Aug. 2016. doi: 10.1109/TAP.2016.2570235
- [16] X. Li, X. Chen, J. Zhang, Y. Liang, and Y. Liu, "Capacity analysis of  $\alpha$ - $\eta$ - $\kappa$ - $\mu$  fading channels," *IEEE Commun. Lett.*, vol. 21, no. 6, pp. 1449–1452, Jun. 2017. doi: 10.1109/LCOMM.2017.2672960
- [17] A. A. dos Anjos, T. R. R. Marins, R. A. A. de Souza, and M. D. Yacoub, "Higher order statistics for the  $\alpha$ - $\eta$ - $\kappa$ - $\mu$  fading model," *IEEE Trans. Veh. Technol.*, vol. 66, no. 6, pp. 3002–3016, Jun. 2018. doi: 10.1109/TAP.2018.2819882
- [18] A. Mathur, Y. Ai, M. R. Bhatnagar, M. Cheffena, and T. Ohtsuki, "On physical layer security of  $\alpha$ - $\eta$ - $\kappa$ - $\mu$  fading channels," *IEEE Commun. Lett.*, vol. 22, no. 10, pp. 2168–2171, Oct. 2018. doi: 10.1109/LCOMM.2018.2860020
- [19] A. Goswami and A. Kumar, "Performance analysis of multi-hop wireless communication systems over  $\alpha$ - $\eta$ - $\kappa$ - $\mu$  channel," *Physical Commun.*, 2018. [Online]. Available: <https://doi.org/10.1016/j.phycom.2018.12.004>
- [20] V. M. Rennó, R. A. A. de Souza, and M. D. Yacoub, "On the generation of  $\alpha$ - $\eta$ - $\kappa$ - $\mu$  samples with applications," in *IEEE 28th Symp. on Personal, Indoor, and Mobile Radio Commun. (PIMRC)*, Oct. 2017. doi: 10.1109/PIMRC.2017.8292358. ISSN 2166-9589 pp. 1–5.
- [21] —, "On the generation of white samples in severe fading conditions," *IEEE Commun. Lett.*, vol. 23, no. 1, pp. 180–183, Jan. 2019. doi: 10.1109/LCOMM.2018.2879928
- [22] A. Bagheri, P. C. Sofotasios, T. A. Tsiftsis, A. Shahzadi, and M. Valkama, "AUC study of energy detection based spectrum sensing over  $\eta$ - $\mu$  and  $\alpha$ - $\mu$  fading channels," in *IEEE Int. Conf. on Commun. (ICC)*, Jun. 2015. doi: 10.1109/ICC.2015.7248521. ISSN 1550-3607 pp. 1410–1415.
- [23] A. A. Hammadi, O. Alhussain, P. C. Sofotasios, S. Muhaidat, M. Al-Qutayri, S. Al-Araji, G. K. Karagiannis, and J. Liang, "Unified analysis of cooperative spectrum sensing over composite and generalized fading channels," *IEEE Trans. Veh. Technol.*, vol. 65, no. 9, pp. 6949–6961, Sep. 2016. doi: 10.1109/TVT.2015.2487320
- [24] S. Kumar, "Performance of ED based spectrum sensing over  $\alpha$ - $\eta$ - $\mu$  fading channel," *Wireless Personal Commun.*, Apr. 2018. [Online]. Available: <https://doi.org/10.1007/s11277-018-5677-6>
- [25] S. Alam, O. Olabiyi, O. Odejide, and A. Annamalai, "A performance study of energy detection for dual-hop transmission with fixed gain relays: area under ROC curve (AUC) approach," in *IEEE 22nd Int. Symp. on Personal, Indoor and Mobile Radio Commun.*, Sep. 2011. doi: 10.1109/PIMRC.2011.6139827. ISSN 2166-9570 pp. 1840–1844.
- [26] P. C. Sofotasios, E. Rebeiz, L. Zhang, T. A. Tsiftsis, D. Cabric, and S. Freear, "Energy detection based spectrum sensing over  $\kappa$ - $\mu$  and  $\kappa$ - $\mu$  extreme fading channels," *IEEE Trans. Veh. Technol.*, vol. 62, no. 3, pp. 1031–1040, Mar. 2013. doi: 10.1109/TVT.2012.2228680
- [27] S. Atapattu, C. Tellambura, and H. Jiang, "Energy detection of primary signals over  $\eta$ - $\mu$  fading channels," in *Int. Conf. on Industrial and Information Systems (ICIS)*, Dec. 2009. doi: 10.1109/ICI-INF.2009.5429879. ISSN 2164-7011 pp. 118–122.
- [28] A. Shahini, A. Bagheri, and A. Shahzadi, "A unified approach to performance analysis of energy detection with diversity receivers over Nakagami- $m$  fading channels," in *Int. Conf. on Connected Vehicles and Expo (ICCVE)*, Dec. 2013. doi: 10.1109/ICCVE.2013.6799881. ISSN 2378-1289 pp. 707–712.
- [29] M. Aloqlah, "Performance analysis of energy detection-based spectrum sensing in  $\kappa$ - $\mu$  shadowed fading," *Electron. Lett.*, vol. 50, no. 25, pp. 1944–1946, 2014. doi: 10.1049/el.2014.2944
- [30] F. von Glehn and U. S. Dias, "On the AUC analysis in cognitive radio networks over  $\kappa$ - $\mu$  fading channel with noise uncertainty," in *Int. Telecom. Symp. (ITS)*, Aug. 2014. doi: 10.1109/ITS.2014.6948024
- [31] —, "Performance analysis of cognitive radio networks over  $\kappa$ - $\mu$  fading channel with noise uncertainty," in *IEEE Radio and Wireless Symposium (RWS)*, Jan. 2014. doi: 10.1109/RWS.2014.6830090. ISSN 2164-2958
- [32] W. A. Silva, K. M. Mota, and U. S. Dias, "Spectrum sensing over Nakagami- $m$ /gamma composite fading channel with noise uncertainty," in *IEEE Radio and Wireless Symposium (RWS)*, Jan. 2015. doi: 10.1109/RWS.2015.7129759. ISSN 2164-2958
- [33] F. F. Digham, M. S. Alouini, and M. K. Simon, "On the energy detection of unknown signals over fading channels," *IEEE Trans. Commun.*, vol. 55, no. 1, pp. 21–24, Jan. 2007. doi: 10.1109/TCOMM.2006.887483
- [34] G. Amir and S. S. Elvino, "Opportunistic spectrum access in fading channels through collaborative sensing," *J. of Commun.*, vol. 2, no. 2, pp. 71–82, Mar. 2007.
- [35] I. Gradshteyn and I. Ryzhik, *Tables of Integrals, Series, and Products*. New York: Academic Press, 1980.
- [36] J. Marcum, "A statistical theory of target detection by pulsed radar," *IRE Trans. on Inform. Theory*, vol. 6, no. 2, pp. 59–267, 1960. doi: 10.1109/TIT.1960.1057560
- [37] S. Atapattu, C. Tellambura, and H. Jiang, "Analysis of area under the ROC curve of energy detection," *IEEE Trans. Wireless Commun.*, vol. 9, no. 3, pp. 1216–1225, Mar. 2010. doi: 10.1109/TWC.2010.03.091085
- [38] T. Fawcett, "An introduction to ROC analysis," *Pattern Recognition Lett.*, vol. 27, no. 8, pp. 861–874, 2006. [Online]. Available: <https://doi.org/10.1016/j.patrec.2005.10.010>
- [39] A. Bagheri, P. C. Sofotasios, T. A. Tsiftsis, A. Shahzadi, S. Freear, and M. Valkama, "Area under ROC curve of energy detection over generalized fading channels," in *IEEE 26th Annu. Int. Symp. on Personal, Indoor, and Mobile Radio Commun. (PIMRC)*, Aug. 2015. doi: 10.1109/PIMRC.2015.7343380 pp. 656–661.
- [40] M. D. Yacoub, "The  $\kappa$ - $\mu$  distribution and the  $\eta$ - $\mu$  distribution," *IEEE Trans. Antennas Propag.*, vol. 49, no. 1, pp. 68–81, Feb. 2007. doi: 10.1109/MAP.2007.370983
- [41] S. Atapattu, C. Tellambura, and H. Jiang, *Energy detection for spectrum sensing in cognitive radio*. Springer, 2014.



**Vanessa Mendes Rennó** was born in Brazil in 1993. He received the B.S.E.E. and the M.Sc. degrees from the National Institute of Telecommunication (INATEL), Brazil, in 2016 and 2018, respectively. Currently is Ph.D. student at University of Campinas (UNICAMP), Campinas, Brazil. Her fields of interest include digital communications, channel coding, wireless communications, channel modeling and simulation, non-linear systems and spectrum sensing, which are the topics she has published scientific papers.



**Rausley Adriano A. de Souza** was born in Brazil in 1972. He received the B.S.E.E. and the M.Sc. degrees from the National Institute of Telecommunication (INATEL), Brazil, in 1994 and 2002, respectively, and the Ph.D. degree from School of Electrical and Computer Engineering of the State University of Campinas (UNICAMP), Campinas, Brazil. From 1995 to 2001, he worked as a Purchase Manager at Leucotron Equipamentos Ltda. He joined the National Institute of Telecommunication, INATEL, in 2002, where he is a Full Professor. He is

presently a Productivity Research Fellow of the National Council for Scientific and Technological Development (CNPq, Brazil). Since 2015 he has been working at the Radiocommunication Reference Center, whose researches are concentrated on the fifth-generation (5G) systems. He has coauthored the book entitled *Digital Transmission - Principles and Applications* (Erica, 2014) in Portuguese. He is a Member of the Brazilian Telecommunications Society (SBrT) and is a Member of the IEEE. His general research interests include wireless communications, fading channel modeling and simulation, diversity systems, and spectrum sensing in cognitive radio systems.



**Michel Daoud Yacoub** was born in Brazil in 1955. He received the B.S.E.E. and M.Sc. degrees from the School of Electrical and Computer Engineering, University of Campinas (UNICAMP), Campinas, Brazil, in 1978 and 1983, respectively, and the Ph.D. degree from the University of Essex, Colchester, U.K., in 1988. He was a Research Specialist with the Research and Development Center, Telebrás, Rio de Janeiro, Brazil, from 1978 to 1985, where he was involved in the development of the Trópico digital exchange family. He joined the School of Electrical

and Computer Engineering, UNICAMP, in 1989, where he is currently a Full Professor. He consults for several operating companies and industries in the wireless communications area. He has authored the books entitled *Foundations of Mobile Radio Engineering* (CRC, 1993) and *Wireless Technology: Protocols, Standards, and Techniques* (CRC, 2001), and coauthored the book entitled *Telecommunications: Principles and Trends* (Erica, 1997) in Portuguese. He holds two patents. His current research interests include wireless communications.